






**MAIN TEXT**

# In vivo peripheral nerve activation using sinusoidal low-frequency alternating currents

Awadh Alhawwash<sup>1,2</sup>  | M. Ivette Muzquiz<sup>3</sup>  | Lindsay Richardson<sup>3</sup> |  
Christian Vetter<sup>3</sup> | Macallister Smolik<sup>4</sup> | Adam Goodwill<sup>5</sup>  | Ken Yoshida<sup>3</sup>  

<sup>1</sup>Weldon School of Biomedical Engineering, Purdue University, West Lafayette, Indiana, USA

<sup>2</sup>Biomedical Technology Department, King Saud University, Riyadh, Saudi Arabia

<sup>3</sup>Department of Biomedical Engineering, Indiana University - Purdue University Indianapolis, Indianapolis, Indiana, USA

<sup>4</sup>Department of Biology, Indiana University - Purdue University Indianapolis, Indianapolis, Indiana, USA

<sup>5</sup>Department of Integrative Medical Sciences, Northeast Ohio Medical University, Rootstown, Ohio, USA

**Correspondence**

Ken Yoshida, Department of Biomedical Engineering, Indiana University - Purdue University Indianapolis, 723 W. Michigan St. SL 220F, Indianapolis, IN 46202, USA.  
Email: [yoshidak@iupui.edu](mailto:yoshidak@iupui.edu)

**Funding information**

This work was funded through a NIH Traiblazer R21 grant (R21EB028469)

**Abstract**

**Background:** The sinusoidal low-frequency alternating current (LFAC) waveform was explored recently as a novel means to evoke nerve conduction block. In the present work, we explored whether increasing the amplitude of the LFAC waveform results in nerve fiber activation in autonomic nerves. *In-silico* methods and preliminary work in somatic nerves indicated a potential frequency dependency on the threshold of activation. The Hering-Breuer (HB) reflex was used as a biomarker to detect cervical vagus nerve activation.

**Methods:** Experiments were conducted in isoflurane-anesthetized swine ( $n = 5$ ). Two stimulating bipolar cuff electrodes and a tripolar recording cuff electrode were implanted on the left vagus nerve. To ensure the electrical stimulation affects only the afferent pathways, the nerve was crushed caudal to the electrodes to eliminate cardiac effects. (1) Standard pulse stimulation ( $V_{stim}$ ) using a monophasic train of pulses was applied through the caudal electrode to elicit HB reflex and to identify the activated nerve fiber type. (2) Continuous sinusoidal LFAC waveform with a frequency ranging from 5 through 20 Hz was applied to the rostral electrode without  $V_{stim}$  to explore the activation thresholds at each LFAC frequency. In both cases, the activation of nerve fibers was detected by a HB reflex-induced reduction in the breathing rate.

**Results:** LFAC was found to be capable of eliciting an HB response. The LFAC activation thresholds were found to be frequency-dependent. The HB threshold was  $1.02 \pm 0.3 \text{ mA}_p$  at 5 Hz,  $0.66 \pm 0.3 \text{ mA}_p$  at 10 Hz, and  $0.44 \pm 0.2 \text{ mA}_p$  at 20 Hz. In comparison, it was  $0.7 \pm 0.47 \text{ mA}$  for a  $100 \mu\text{s}$  pulse. The LFAC amplitude was within the linear limits of the electrode interface. Damage to the cuff electrodes or the nerve tissues was not observed. Analysis of  $V_{stim}$ -based compound nerve action potentials (CNAP) indicated that the decrease in breathing rate was found to be correlated with the activation of slower components of the CNAP suggesting that LFAC reached and elicited responses from these slower fibers associated with afferents projecting to the HB response.

This is an open access article under the terms of the [Creative Commons Attribution-NonCommercial-NoDerivs](https://creativecommons.org/licenses/by-nc-nd/4.0/) License, which permits use and distribution in any medium, provided the original work is properly cited, the use is non-commercial and no modifications or adaptations are made.

© 2022 The Authors. *Artificial Organs* published by International Center for Artificial Organ and Transplantation (ICAOT) and Wiley Periodicals LLC.



**Conclusions:** These results suggest the feasibility of the LFAC waveform at 5, 10, and 20 Hz to activate autonomic nerve fibers and potentially provide a new modality to the neurorehabilitation field.

**KEYWORDS**

electrical stimulation, Hering–Breuer reflex, low-frequency alternating current, nerve activation, neuromodulation, vagus nerve stimulation

## 1 | INTRODUCTION

Electrical stimulation of the autonomic nervous system (ANS) using standard pulse stimulation is a means to achieve therapeutic outcomes for the ANS and modulation of major organ function. Pulse stimulation of the cervical vagus nerve (VNS) is one approach currently being applied to achieve therapeutic outcomes. As VNS became clinically approved to treat epilepsy<sup>1</sup> and depression,<sup>2,3</sup> a tremendous number of techniques emerged to modulate the vagus nerve responsible for the treatment of obesity,<sup>4</sup> respiratory,<sup>5</sup> and inflammatory<sup>6</sup> diseases and regulation of cardiac abnormalities,<sup>7</sup> among others. As the vagus nerve mediates different organ functions, it contains nerve fibers of different populations based on the caliber size, function (sensory and motor), and structure (unmyelinated and myelinated).<sup>8</sup> Therefore, selective VNS to modulate the nerve response is desired to enable titration of stimulation and optimization of modulation targeting specific organ systems.

The Hering-Breuer reflex (HB) is one of many reflexes mediated by the nerve fibers in the vagus nerve.<sup>9–11</sup> It is thought to be a mechanism to compensate for the over-inflation of the lung. When the lung is over-inflated, pulmonary stretch receptors transmit inhibitory signals to the Central Nervous System (CNS) via activation fibers in the vagal afferent pathway. The reflex results in an inhibition of inspiration depth and frequency. The reflex volley is manifested in changes to the breathing rhythm, effected by motor nerve fibers projecting from the pontine respiratory center through the phrenic nerve and spinal nerves to the intercostal muscles. As a result, the respiratory center maintains a normal inspiration/expiration mechanism and prevents lung inflation.<sup>9–11</sup> When electrically stimulating the vagus nerve to induce the HB reflex, the breathing rate decreases as a result of modulating the neural activity carried by the vagus nerve afferent fibers.<sup>12,13</sup> However, if the stimulation activates nerve fibers, off-target efferent fibers such as cardiac efferents within the vagus nerve bradycardia<sup>14,15</sup> can result.

The historical use of the rectangular pulse waveforms for electrical stimulation (activation) has provided an adequate means to induce nerve activity at the intra and extracellular levels of nerve stimulation. However, the conventional rectangular pulse waveform preferentially activates large-caliber nerve fibers before small nerve

fibers,<sup>16</sup> which limits target selectivity. Therefore, alternative methods for selective activation are emerging to expand the toolset available for the neuromodulation field.

Several methods to selectively activate and block nerve fibers have been developed and investigated, which rely on optimizing the stimulation waveform parameters to induce selective block of a target population of nerve fibers while maintaining the activity of other populations. Such optimization resulted in different waveforms that utilize the blocking effect to selectively activate nerve fibers, such as anodal block,<sup>17</sup> sub-threshold prepulse,<sup>18</sup> ramp prepulse,<sup>19</sup> exponentially rising waveform,<sup>20</sup> and quasi-trapezoidal waveform.<sup>21,22</sup> Although those methods are effective in the short term, many of these techniques rely on imbalanced charge injection which has longer term nerve injury consequences and will require additional methods and complexities in the stimulation waveform to overcome.

Recently, we reported the feasibility of using a sinusoidal low frequency alternating currents (LFAC) waveform to reversibly block nerve conduction in mammalian autonomic peripheral nerves. In the rat model,<sup>23–25</sup> LFAC presented between VNS and the heart blocked the descending volley to block their effects on the heart effectively blocking VNS elicited bradycardia. Similarly, when applied against the ascending VNS volley that elicits the Hering-Breuer (HB) reflex response,<sup>25,26</sup> the LFAC waveform presented at 1 Hz blocked the afferent nerve activity to block the HB response. As the LFAC waveform is symmetrical, it is intrinsically charge balanced. However, given the low frequencies, electrodes with interfaces capable of passing currents at these frequencies without exceeding the water window need to be used and care needs to be exercised. Although the waveform is still under development, it has been shown to reversely block nerve conduction without onset activation and appears to preferentially block small nerve fibers first.<sup>23,25,26</sup>

Studies utilizing or exploring sinusoidal waveforms have been reported in the literature,<sup>27–31</sup> and the waveform frequency varies widely based on their applications. The characteristics of the sinusoidal LFAC waveform, being at low frequency, not at DC, pure tone continuous wave, symmetrical, and charge balance, could be utilized to achieve an optimal stimulation protocol. In terms of neural excitability, waveform frequency, electrode geometry, type, and material play major roles in determining



the overall neural response to stimuli.<sup>32</sup> Therefore, those factors in accordance with the cellular axonal cable properties,<sup>33</sup> length, and time constants, can be modulated to provide neural excitation with limited risks associated with damage to tissue and the electrode interface.

In this study, we aim to (1) explore and provide experimental evidence that the LFAC waveform is able to activate ANS nerve fibers within mammalian cervical vagus nerve using the HB reflex as a biomarker, and (2) determine whether the threshold of activation is a function of the applied LFAC frequency.

## 2 | METHODS

### 2.1 | Animal preparation and electrodes configuration

All experiments in this study were approved by the Institutional Animal Care and Use Committee (IACUC) at the Indiana University School of Medicine (IUSM IACUC) and performed in accordance with the Guide

for the Care and Use of Laboratory Animals (National Institutes of Health Publication. No. 85–23, Revised 2011 in Ref. [34]). These experiments were conducted following the LFAC block experiments described in “*In vivo application of low-frequency alternating currents on porcine cervical vagus nerve evokes reversible nerve conduction block*” using the same animals and detailed surgical and preparation methods are published in Refs. [25,26].

Briefly, the left cervical vagus nerves of five adult male domestic Landrace swine (~50 kg) were isolated bilaterally following sedation and continuous isoflurane anesthesia. Anesthesia was maintained at the surgical plane throughout the experiment. Figure 1 illustrates the in-vivo experimental setup and electrode placement. Vital signs were continuously monitored during the experiment and breathing change was measured through a pressure transducer cuff placed around the animal's chest. Two bipolar cuff electrodes were placed on the isolated nerve; a caudal electrode (CE) was used for vagal pulse stimulation and a rostral electrode (RE) was used for LFAC stimulation. Both electrodes were Pt-Ir bipolar

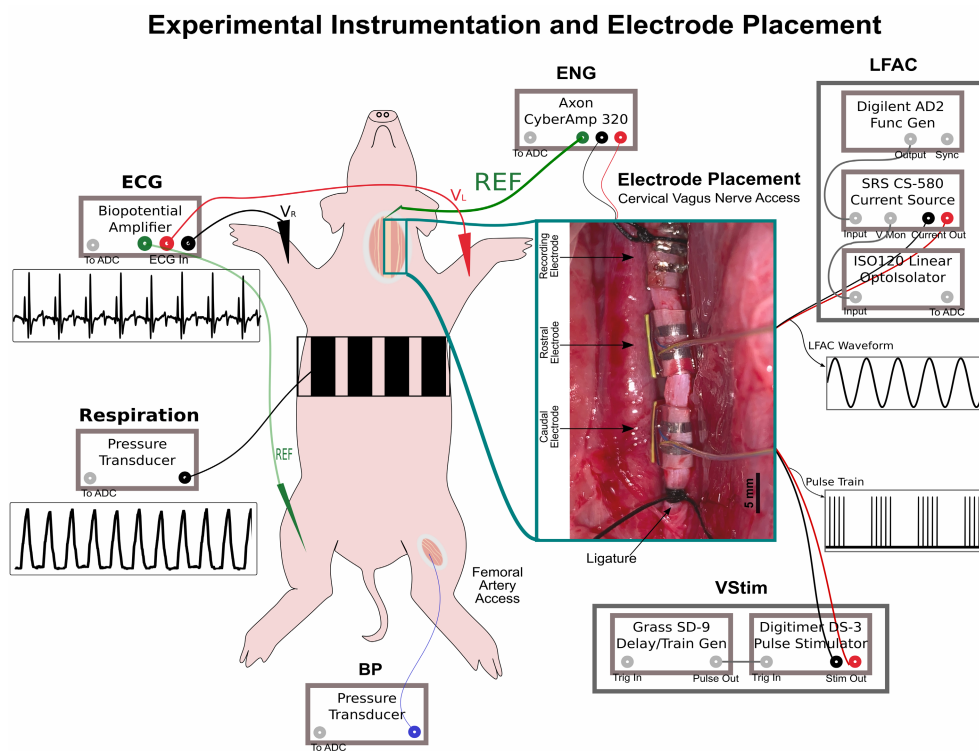


**FIGURE 1** An illustration of the experimental instrumentation and electrode placement. The site of the cervical vagus nerve access displays the three electrodes with respect to the animal position. Standard pulse vagal nerve stimulation (Vstim) was delivered through the caudal electrode (CE), LFAC waveform was delivered through rostral electrode (RE). Tripolar recordings of the ENG were obtained from the recording electrode, placed most rostral. Respiration rates were measured using a pressure transducer cuff placed around the animal's chest. The image also shows the ligature used to crush the nerve most caudal to eliminate the cardiac effects of the Vstim. [Color figure can be viewed at [wileyonlinelibrary.com](http://wileyonlinelibrary.com)]



cuff electrodes (CorTec GmbH, Freiburg, Germany) coated with polyethylenedioxythiophene (PEDOT)-based Ampliccoat® (Heraeus Medical Components, Saint Paul MN). A custom-made tripolar cuff electrode was placed most rostral for electroneurograph (ENG) signal.<sup>35</sup> The cardiac effect was eliminated via crushing the nerve caudal to the most caudal electrode using a ligature. The crush is similar to a caudal vagotomy, where the stimulation affects the afferent pathways only.<sup>14</sup> All electrodes and implants were applied unilaterally on the left cervical vagus. The right cervical vagus was left untouched and helped maintain the stability of the preparation. The recording and stimulation instrumentation used in this study were the same as in Refs. [25,26]. The only major difference was the stimulation paradigm used.

## 2.2 | Nerve stimulation and experimental paradigm

### 2.2.1 | Pulse stimulation

The first part of the experiment was conducted to elicit HB reflex and to identify the activated nerve fiber type. A monophasic train of 5 pulses (2 Hz pulse train rate) was applied to the vagus nerve, with a cathodic pulse width of 100  $\mu$ sec, 200 ms train duration, and 25 Hz pulse rate. The pulses were presented to the CE using an optoisolated stimulator (DS3, Digitimer LTD, Hertfordshire UK) triggered by a square pulse stimulator (Grass SD9, Grass Instrument, Quincy, Massachusetts, USA). The pulse amplitude was gradually increased with simultaneous measurements of changes in inter-breath intervals to determine the activation of the HB reflex. ENG signal was measured and recorded with a gain of x50k and prefiltered with a high-pass filter at 300 Hz (Cyberamp 320, Axon Instruments, Foster City, CA).

### 2.2.2 | LFAC stimulation

The LFAC waveform was generated as a continuous sinusoidal waveform using an arbitrary function generator (Analog Discovery 2, Digilent Inc, Pullman WA) and controlled by a tuning application written in LabVIEW®. The LFAC waveform was delivered to the RE via a custom-built analog optical isolator followed by an isolated voltage-controlled current source (CS580, SRS: Stanford Research Systems) with a constant gain of 1 mA per Volt. The LFAC stimuli were applied using three frequencies: 5, 10, and 20 Hz. In one experiment, the LFAC frequency was increased to 100 and 500 Hz. With each frequency, the

LFAC stimuli were applied at different amplitudes and each stimulation amplitude lasted for about 20 seconds and was followed by a zero-amplitude period to allow for breathing recovery. Because the activation of HB reflex has the potential to elicit apnea, and complete stoppage of animal breathing, the periods of LFAC application were kept at minimum.

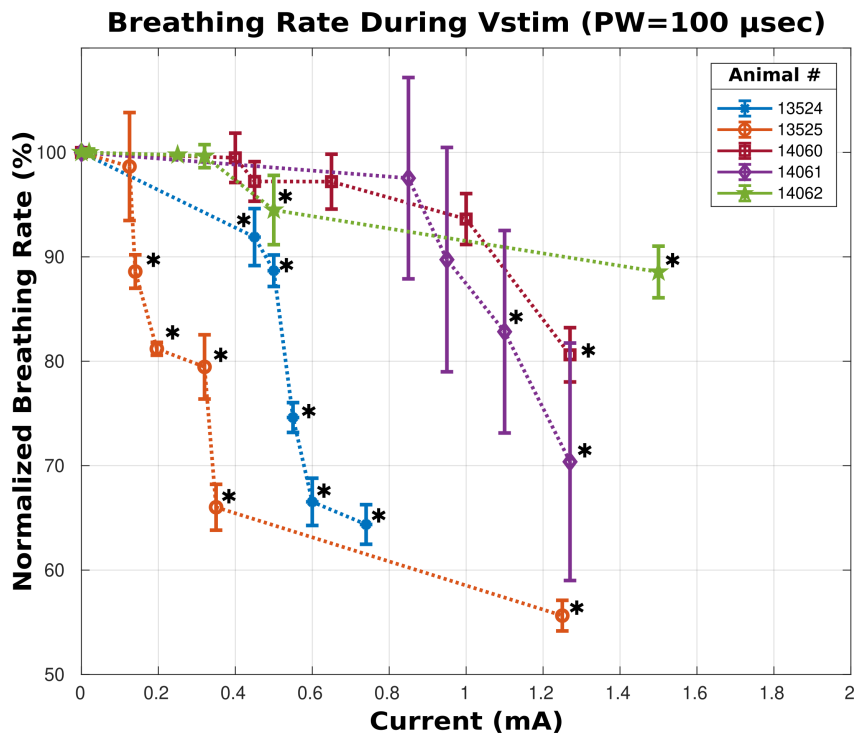
Moreover, during LFAC application, the voltage drops across the RE were measured continuously via the calibrated monitored output of the current source. This allowed to monitor and maintain the linearity of the input current and output voltage across the electrode as an indication of the maximum current to be applied without exceeding the cell potentials causing the hydrolysis of water or the “water window.” For PEDOT coated electrode, the water window reported as a half-cell potential against a standard Ag/AgCl electrode is  $-0.9$  to  $0.6$  V.<sup>32</sup> Thus, the corresponding full cell potential is  $\sim 1.5$  V. Additionally, the change in inter-breath intervals was measured simultaneously to visualize changes in breathing rate indicating the activation of the HB reflex.

## 2.3 | Data analysis

The analysis of both modes of stimulation was performed in MATLAB® (Version: R2018b, The MathWorks). The instantaneous breathing rates during the baseline (initial period before stimulation) and stimulation were calculated by measuring the time between each inspiration peak from the respiration data. Because the baseline breathing rate was different for each animal, the instantaneous breathing rate was normalized to the average instantaneous breathing rate during the baseline of each run. During Vstim, the threshold of activation was identified as the lowest pulse amplitude that caused an increase in the intervals between breathing peaks. During LFAC stimulation, the frequency and current amplitude to peak ( $\text{mA}_p$ ) were quantified. The LFAC waveform was applied through a bipolar electrode. The current flows from contact to contact and the potential spanning the electrodes relates to the full electrochemical cell potential. At any given phase of the sinusoidal waveform, the relevant cell potential is the potential across the cell, the relevant current the current between the contacts, and not the peak-to-peak value of the sinusoid. Thus, we report the current amplitude-to-peak value rather than the peak-to-peak value of the sinusoid.

Furthermore, during Vstim, Compound Nerve Action Potentials (CNAPs) were extracted from the ENG signal using spike-triggered averaging in a 6 ms window of interest. Heavy in-band noise interference from the SRS current source obscured the ENG signal and prevented

**FIGURE 2** Normalized breathing rate percentages as a function of stimulus intensity during Vstim with 100  $\mu$ sec pulse width. The error bars indicate standard deviations between the instantaneous breathing rates. Asterisks represent a significant reduction ( $p$ -value  $< 0.05$ ) compared to baseline. [Color figure can be viewed at [wileyonlinelibrary.com](http://wileyonlinelibrary.com)]



recovery of the instantaneous ENG recordings. Therefore, the quantification of CNAP peaks and estimation of conduction velocity were based on stimulus-triggered averages of the ENG recordings. In this analysis, the evoked CNAP peak latency was calculated as the time difference between CNAP peaks to the rising edge of the stimulation artifact. The conduction velocity of each peak was calculated with respect to the distance from the first contact of the stimulating electrode to the center contact of the tripolar recording electrode. The ECG signal was digitally filtered from 1 Hz to 40 Hz, and the heart rate during stimulation was calculated based on the instantaneous R-R interval, averaged with a 5 s moving average filter.

## 2.4 | Statistical analysis

A one-way ANOVA with Dunnett's multi-comparison test was used to determine the effect of pulse amplitude of Vstim on breathing rate ( $n = 5$ ). Furthermore, a two-way ANOVA with Tukey's multi-comparison test was used to determine the effects of LFAC amplitudes and frequency on breathing rate ( $n = 5$ ). Because of the variation of different LFAC amplitudes applied during the experiments, we grouped the data into four treatments (No stim, below threshold, at threshold, and above threshold) and two factors (amplitude and frequency). To avoid bias during grouping, each experiment's results were analyzed using one-way ANOVA to determine the threshold resulting in a significant reduction in breathing rate ( $p$ -value  $< 0.05$ ). Additionally, a one-way ANOVA with Dunnett's

multi-comparison test was used to determine the effect of LFAC frequency (5, 10, and 20 Hz only) on the thresholds to reach LFAC activation. In this test, each experimental current to peak thresholds was normalized to their 5 Hz thresholds. In all comparisons, statistically significant differences were determined when  $p$ -values are  $< 0.05$ . All statistical analyses were performed using GraphPad Prism software version 9.0 (Graphpad Software, Inc) and MATLAB.

## 3 | RESULTS

Measurements of the breathing rate were used as the main physiological response indicator. During Vstim, clear HB responses were detected. The threshold for a sustained HB varied between experiments, but the mean threshold that resulted in a significant reduction in breathing rate ( $p$ -value  $< 0.05$ ) was within the range of  $0.7 \pm 0.47$  mA (mean  $\pm$  SD) using a 100  $\mu$ sec pulse. Figure 2 shows the normalized breathing rate percentages as stimulus intensity increases.

Stimulus-triggered averages of simultaneously measured ENG clearly show that later peaks of the CNAP associated with larger pulse amplitudes correlate with the decreased breathing rate related to the HB reflex. Figure 3 (from animal# 14062) shows that as the Vstim intensity increased, two distinct CNAP peaks were observed. The first "fast" peak (average conduction velocity of 47.0 m/s) with a threshold of  $0.29 \pm 0.06$  mA had no effect on the respiration rate. However, the shallow breathing and reduced

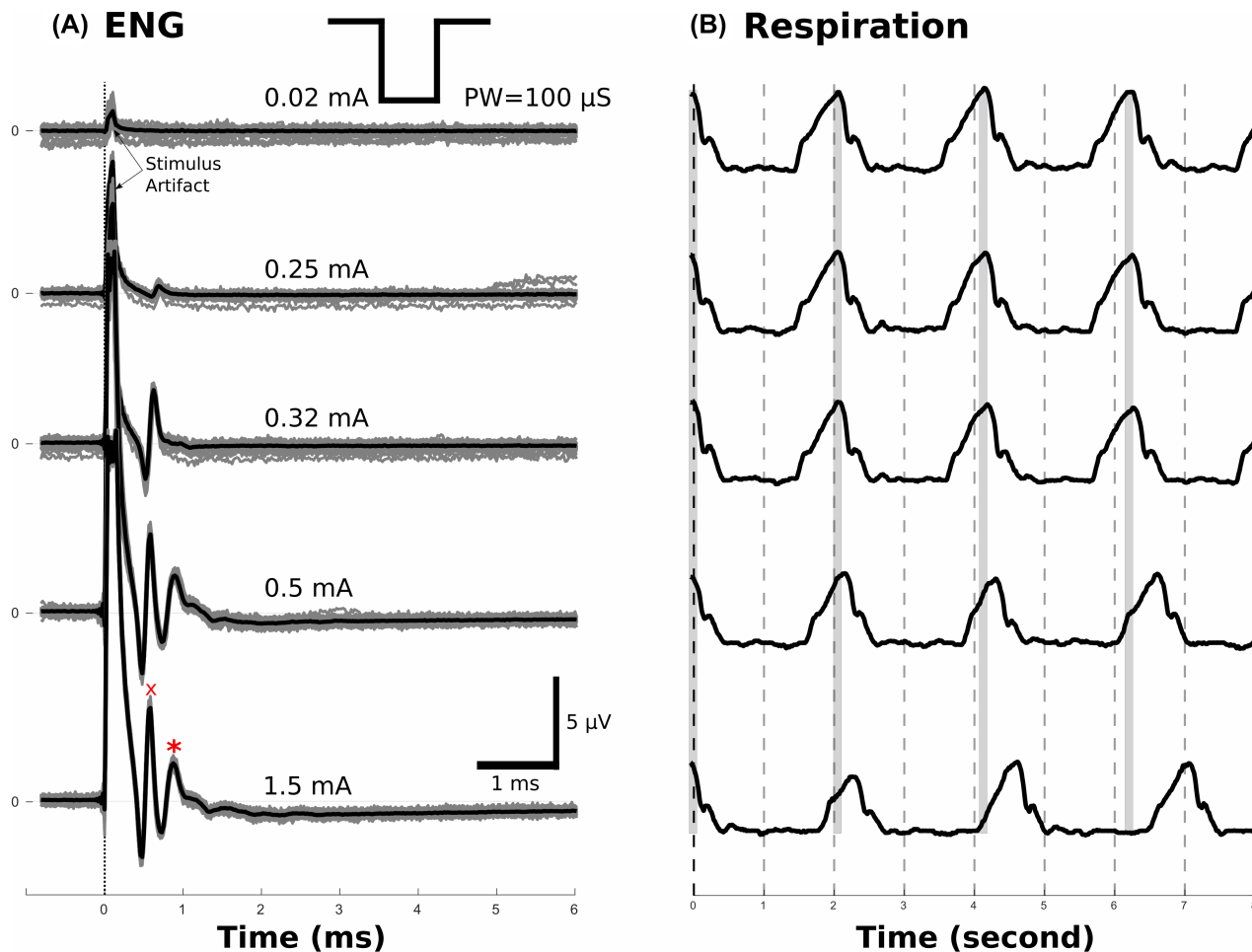


**FIGURE 3** An example of the ENG recording during Vstim at multiple stimulation amplitudes and the corresponding respiration behavior during each run. (A) Stimulation-triggered averages of ENG evoked by Vstim amplitudes: 0.02, 0.25, 0.32, 0.5, and 1.5 mA. The fast CNAP peak (marked with X) appeared at 0.25 mA with an average conduction velocity of 47 m/s and the slower peak (marked with \*) appeared at 0.5 mA with a conduction velocity of 29 m/s. (B) The respiration behavior during 8 seconds of Vstim at each corresponding amplitude. The respiration peaks are aligned to show the variation in the inner breathing intervals indicating the activation of the HB reflex. The ordinate of respiration is an arbitrary unit.

respiration rate was associated with the presence of the second “slow” peak of the CNAP (average conduction velocity of 29.0 m/s) evoked with higher pulse amplitudes at a threshold of  $0.45 \pm 0.10$  mA. From Figure 2, amplitude ( $\geq 0.5$  for animal #14062) resulted in a significant reduction in breathing rate compared to baseline, which was the threshold of observing the slower CNAP seen in Figure 3A. Due to heavy in-band noise interference from the current source, CNAP was only retrieved from two experiments; therefore, no statistical comparison between breathing rate reduction and the presence of CNAP peaks was performed.

Presentation of the LFAC waveform instead of pulse stimulation also resulted in a HB response. Figure 4A shows a representative continuous recording of the breathing change during the application of a 5 Hz LFAC waveform at different LFAC amplitudes, 2nd trace. The 3rd trace shows the instantaneous calculated breathing rate

per minute based on the time intervals between each adjacent breathing peak. As the LFAC amplitude increases, the breathing rate decreases further until a state of near apnea is reached at an amplitude of 1.5 mA<sub>p</sub>. The recovery time between each LFAC increment was observed to resume the normal breathing as shown in the calculated breathing rate. As expected, the HB-reflex resulted in a larger time interval between the breathing peaks and further increments of LFAC amplitude would result in a complete stoppage of breathing. The bottom trace showing the instantaneous heart rate during this experimental sequence indicates that there were no cardiac changes during the application of LFAC. The missing effect on the heart is assumed to be due to the caudal crush of the nerve eliminating descending volleys caudal to the ligature.

Similar results as those shown in Figure 4A were obtained using 10 and 20 Hz LFAC. However, the HB activation thresholds were lower than at 5 Hz. As shown in

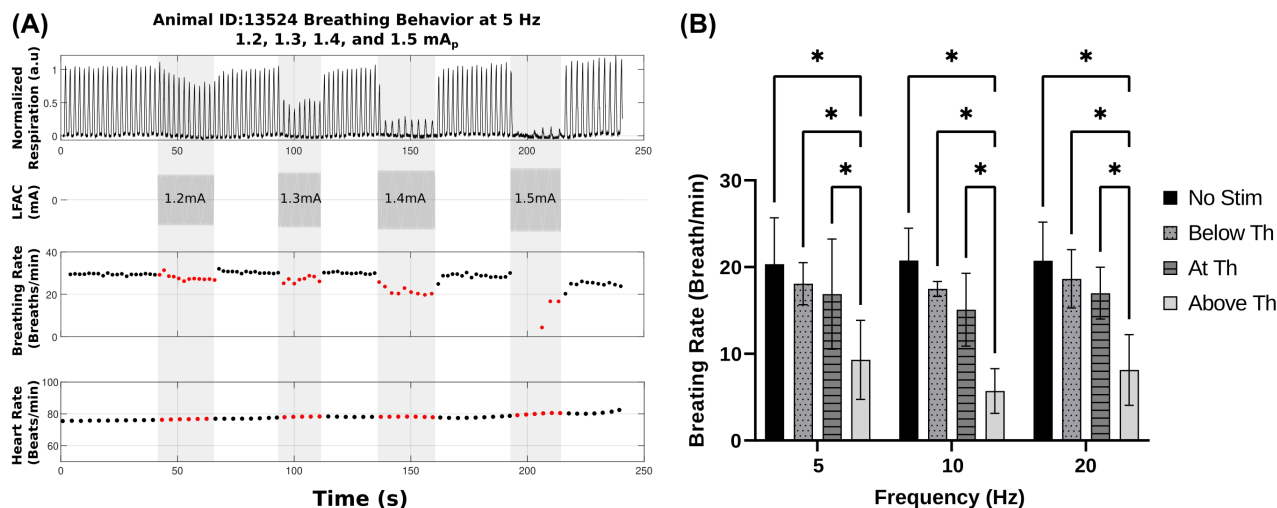


**FIGURE 4** (A) The effect on the breathing rate and amplitude during 5 Hz LFAC stimulation at different amplitudes shown in the shaded regions: 1.2, 1.3, 1.4, and 1.5 mA<sub>p</sub>. The panels show a continuous experimental sequence where LFAC was applied at different amplitudes while simultaneously measuring respiration, plotting respiration rate, and heart rate. The respiration panel shows the respiration peaks used in calculating the instantaneous breathing rate. The breathing rate panel shows the instantaneous breathing rate (breaths/min) changes as the LFAC waveform is applied at different amplitudes. The heart rate panel shows the 5-second averaged heart rate in beats per min. (B) Summary of the two-way ANOVA analysis showing the effect of LFAC amplitude and frequency on breathing rate. There was no significant difference between frequencies ( $F [2, 43] = 0.6444$ ,  $p$ -value = 0.5300); however, significant differences were found between amplitudes (\* $p$ -value < 0.05). [Color figure can be viewed at [wileyonlinelibrary.com](http://wileyonlinelibrary.com)]

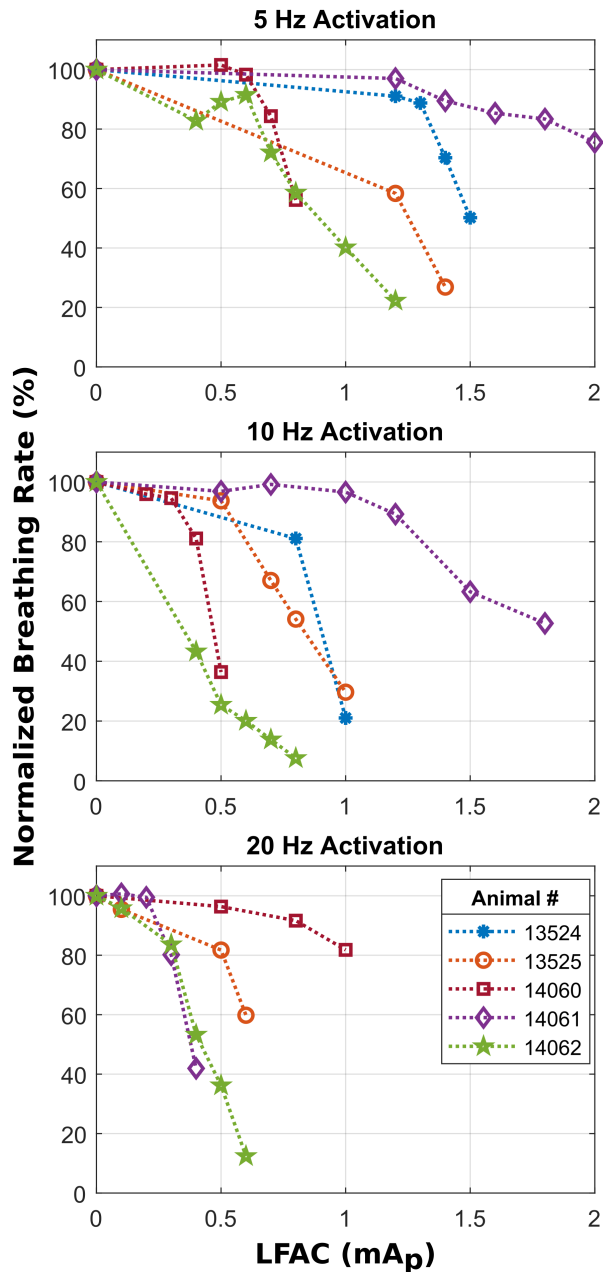
Figure 5, the normalized breathing rate percentages tend to decrease at higher intensities and higher waveform frequencies. The maximum reduction in breathing rate of each animal required higher intensity, however, with higher frequencies, lower intensity is required to reach the same maximum reduction. Figure 4B shows a summary of the two-way ANOVA with Tukey's multi-comparison test used to determine the effects of LFAC amplitudes and frequency (5, 10, and 20 only) on breathing rate. The results indicate that there was a significant reduction in breathing rate ( $p$ -value < 0.05) due to conditioning at different levels of LFAC amplitudes. However, there was no significant difference due to different LFAC frequencies ( $F [2, 43] = 0.6444$ ,  $p$ -value = 0.5300). Additionally, the interaction between LFAC amplitude and frequency was not significant ( $F [6, 43] = 0.2196$ ,  $p$ -value = 0.9684).

Figure 6A displays that all animals showed the same activation threshold decreasing trend, which shows the inverse relationship between LFAC activation threshold and waveform frequency. These experimental threshold curves were constructed based on the minimum LFAC amplitudes that were capable to induce a significant HB-reflex ( $p$ -value < 0.05). In Figure 6B, we normalized the activation threshold curves to better illustrate the effect of frequency on the activation threshold. Statistically, one-way ANOVA with Dunnett's multi-comparison test revealed that increasing LFAC frequency from 5 Hz to 10 and 20 Hz resulted in a significant reduction in threshold to achieve activation ( $p$ -value < 0.05). In one experiment,

we applied 100 and 500 Hz LFAC stimulation to further assess the threshold-frequency dependency and the results revealed even lower activation thresholds

## 4 | DISCUSSION

The first part of these experiments demonstrates the use of Vstim to induce vagal afferent activity. Using breathing rate as a biomarker, the results point to the activation of HB reflex. The results were consistent with previous studies which showed that HB reflex is mediated through the activation of the vagal afferent fibers<sup>11</sup> and that is not only during normal respiration mechanism but also during Vstim.<sup>12,13</sup> Although complete apnea was avoided during Vstim, reaching a 10% reduction in breathing rate required different stimuli strength in different animals, as shown in Figure 2, which could be substantially suprathreshold; therefore, the real threshold range is likely much lower than what we report here. This variation in current thresholds to reach significant HB reflex was most likely due to using different electrodes with different impedance. The elimination of the cardiac effect by crushing the nerve resulted in a rostral elicited afferent activity<sup>14</sup> as there were no observed changes in heart rate during the experiments. Furthermore, the Vstim evoked CNAP peaks, in Figure 3A, in conjunction with the physiological response of respiration, Figure 2, suggests that HB reflex was mediated by the slower nerve fibers.<sup>26,36</sup>



**FIGURE 5** Normalized breathing rate percentages with respect to the averaged breathing rate during baseline. Each result is plotted as a function of the applied LFAC amplitudes with 5 Hz (top), 10 Hz (middle), and 20 Hz (bottom). Only 4 experiments were tested with 20 Hz stimulation. [Color figure can be viewed at [wileyonlinelibrary.com](http://wileyonlinelibrary.com)]

One of our key findings in this study is the capability of the LFAC waveform to induce peripheral nerve activation that results in an end-organ functional change. The activation of the vagal nerve fibers was assessed via direct quantification of the breathing rate as a biomarker indicating the activation of HB reflex. The substantial changes in respiration during LFAC stimulation, slow respiration followed by a slow recovery, as shown in [Figure 4A](#), are consistent with the characteristics of HB reflex activation as reported by [11–13](#)

Additionally, applying the LFAC waveform at 5, 10, and 20 Hz revealed that the activation threshold is frequency-dependent. The higher the LFAC frequency, the lower the stimulation current needed to reach the threshold, as shown in [Figures 5 and 6](#). Moreover, the activation thresholds were within the defined water window of the activation electrode, which resulted in no apparent damage to the nerve or the electrodes themselves. It should be noted that this work was conducted in a large nerve trunk 3–4 mm in diameter. Our prior work in rat vagus [23](#) demonstrated LFAC block in a small 0.5 mm diameter nerve for an efferent pathway biomarker, bradycardia. This was repeated in the large swine nerve against an afferent pathway biomarker, HB reflex. [26](#) The activation work was not conducted contemporaneously with the prior small nerve model. But both activation and block are showing effect in current work in the somatic rat sciatic nerve. [37](#)

Both LFAC-based nerve conduction block and nerve activation were obtained using the same electrode and the same preparation method. LFAC block thresholds are lower than LFAC activation thresholds and are not observed to have a frequency dependence. Current work includes exploring the mechanism behind the frequency dependency. The preliminary results from *in silico* model suggest that the cable properties of nerve fibers, such as length and time constants along with the activation function (which involves the geometry of the electrodes) combine to play a role in this dependency. [38](#) The influence of such parameters directly influences the axon's transmembrane potential, which is determined by potential distributions in both time and space. [33,39](#) In the case of myelinated fibers, spacing of electrode contacts may be tuned to target specific sites around the node of Ranvier, which have different fiber geometry dependency, and therefore influence the ionic channels dynamic for excitation. Understanding the mechanism behind the observed frequency dependency will be useful to enable the tuning of LFAC-based stimulation while limiting the off-target effects.

This feature of LFAC waveform frequency dependency combined with the observation of the independence of LFAC block thresholds to frequency leads to the concept of a Block-Activation window. The window closes with increasing LFAC frequency such that at frequencies above 10 Hz, activation is the dominant effect. These further suggest that the underlying mechanism for LFAC block and LFAC activation are different, a notion that is showing itself in current *in-silico* work exploring LFAC in our lab. [37](#) The nature of the order of LFAC fiber activation is unclear. Unfortunately, in this work, the analog current source's in-band noise obscured the spontaneous nerve activity. Unlike VStim, LFAC did not produce a detectable CNAP. This suggests that LFAC activation may be asynchronous to the





## LFAC Activation Threshold Vs. Frequency

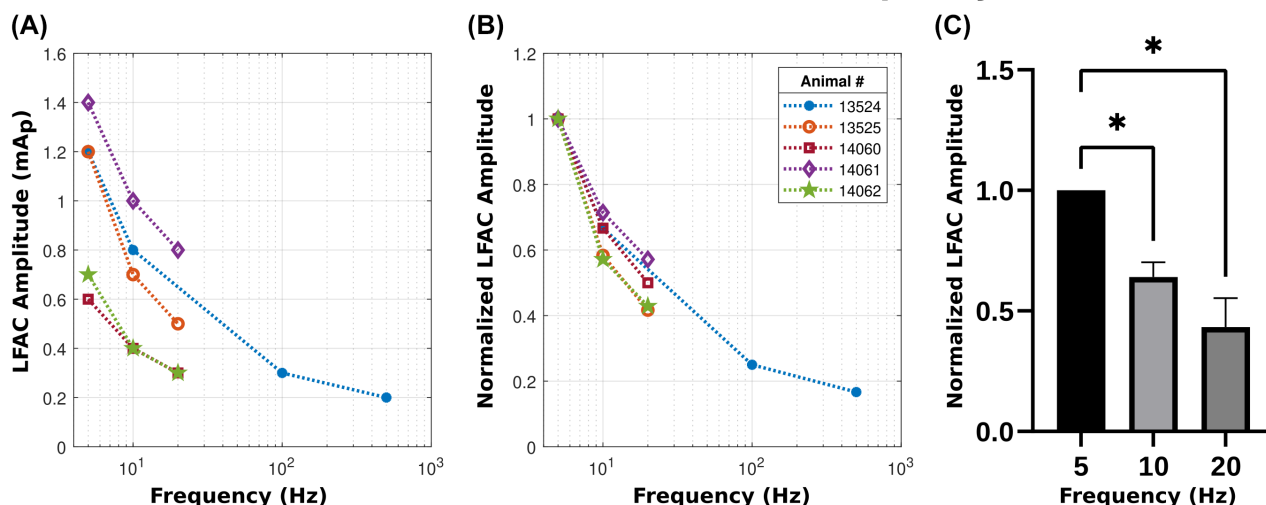


**FIGURE 6** (A) The resulted activation threshold curves as function of the applied LFAC frequency to induce HB-reflex. Each threshold was determined by the minimum applied LFAC amplitude that evoked a steady HB reflex resulting in significant breathing rate reduction ( $p$ -value  $< 0.05$ ). In one experiment, 100 and 500 Hz were applied to test the breathing change at higher frequencies. (B) Normalized activation threshold curves to the 5 Hz thresholds used in the statistical analysis. (C) Summary of one-way ANOVA showing the effect of LFAC frequency (5, 10, and 20 Hz only) on the activation threshold ( $*p$ -value  $< 0.05$ ). [Color figure can be viewed at [wileyonlinelibrary.com](http://wileyonlinelibrary.com)]

sinusoidal waveform and would be a property that distinguishes itself from activation via standard pulse stimulation. Although there is still work to do to understand its mechanism and characterize its block/activation properties, LFAC is a stimulation modality built on a simple waveform that presents itself and tunes between activation and block simply based on the frequency and amplitude of the sinusoidal waveform.<sup>23,24,26,40</sup>

Furthermore, the prior blocking results<sup>23,26</sup> suggested the possibility of the selective block, and this feature might be applied to activate nerve fibers preferentially. Based on the Vstim results, LFAC stimulation might be activating nerve fibers in a size-wise fashion. Therefore, determining the order of fibers recruitment using LFAC is still to be determined as opposed to pulse stimulation. These results are important for LFAC to be a promising new technique to activate peripheral nerve fibers and it is our aim to further investigate the phenomenon with different nerve fibers and biomarkers.

### AUTHORS' CONTRIBUTIONS

AA performed in vivo LFAC activation experiments, wrote analysis scripts, analyzed, and interpreted results, and draft the article. MIM performed in-vivo LFAC block and pulse stimulation experiments, and data collection. LR designed and constructed cuff electrodes and assisted in in-vivo experiments. CV and MS assisted in the surgical placement of the electrodes, and data collection. AG performed a surgical cut down to access the nerve. KY conceived, designed the experiments, and interpreted the results. KY directed the overall work, trained the students on surgical placement and running of the experiment, and

wrote custom MATLAB analysis scripts. All authors reviewed and edited the manuscript.

### ACKNOWLEDGMENTS

The authors acknowledge the generous laboratory support and facilities provided by Dr Johnathan Tune which enabled the successful execution of the animal work. We also acknowledge support from the Familien Hede-Nielsens Fonden which enabled the purchase of the PCB printers used in this project. The authors also acknowledge funding from King Saud University for Alhawsash's scholarship and support from the Department of Biomedical Engineering Research Assistantship program funding Ms Muzquiz, Ms Richardson, and Mr Vetter. The authors also acknowledge Nathaniel Lazorchak for his contribution to generating a custom MATLAB interface to visualize respiration in real-time, and Ryne Horn for his contributions during analysis.

### CONFLICT OF INTEREST

An invention disclosure and US provisional patent (63/244278) were filed for this technique.

### DATA AVAILABILITY STATEMENT

The data that support the findings of this study are available and can be obtained following a reasonable request to the corresponding author.

### ETHICS STATEMENT

All experiments were carried out under a protocol approved by the Indiana University School of Medicine Institutional Animal Care and Use Committee (IUSM



IACUC). They were performed in accordance with the Guide for the Care and Use of Laboratory Animals (National Institutes of Health Publication. No. 85–23, Revised 2011).

## ORCID

Awadh Alhawwash <https://orcid.org/0000-0003-0044-5416>

M. Ivette Muzquiz <https://orcid.org/0000-0002-8657-6101>

Adam Goodwill <https://orcid.org/0000-0003-3701-3713>

Ken Yoshida <https://orcid.org/0000-0003-4566-580X>

## TWITTER

Ken Yoshida @bioellab

## REFERENCES

- Morris GL, Mueller WM. Long-term treatment with vagus nerve stimulation in patients with refractory epilepsy. The Vagus Nerve Stimulation Study Group E01-E05. *Neurology*. 1999 Nov 1;53(8):1731–5.
- Aaronson ST, Sears P, Ruvuna F, Bunker M, Conway CR, Dougherty DD, et al. A 5-year observational study of patients with treatment-resistant depression treated with vagus nerve stimulation or treatment as usual: comparison of response, remission, and suicidality. *Am J Psychiatry*. 2017 Jul 1;174(7):640–8.
- Rush AJ, George MS, Sackeim HA, Marangell LB, Husain MM, Giller C, et al. Vagus nerve stimulation (VNS) for treatment-resistant depressions: a multicenter study. *Biol Psychiatry*. 2000 Feb 15;47(4):276–86.
- Ikramuddin S, Blackstone RP, Brancatisano A, Toouli J, Shah SN, Wolfe BM, et al. Effect of reversible intermittent intra-abdominal vagal nerve blockade on morbid obesity: the ReCharge randomized clinical trial. *JAMA*. 2014 Sep 3;312(9):915–22.
- Agostoni E, Chinnock JE, Daly MDB, Murray JG. Functional and histological studies of the vagus nerve and its branches to the heart, lungs and abdominal viscera in the cat. *J Physiol*. 1957;135(1):182–205.
- Bonaz B, Sinniger V, Hoffmann D, Clarençon D, Mathieu N, Dantzer C, et al. Chronic vagus nerve stimulation in Crohn's disease: a 6-month follow-up pilot study. *Neurogastroenterol Motil*. 2016;28(6):948–53.
- Samniang B, Shinlapawattayatorn K, Chunchai T, Pongkan W, Kumfu S, Chattipakorn SC, et al. Vagus nerve stimulation improves cardiac function by preventing mitochondrial dysfunction in obese-insulin resistant rats. *Sci Rep*. 2016 Feb 1;6(1):19749.
- Yoo PB, Lubock NB, Hincapie JG, Ruble SB, Hamann JJ, Grill WM. High-resolution measurement of electrically-evoked vagus nerve activity in the anesthetized dog. *J Neural Eng*. 2013 Apr 1;10(2):026003.
- Paintal AS. Vagal sensory receptors and their reflex effects. *Physiol Rev*. 1973 Jan;53(1):159–227.
- Widdicombe J. Reflexes from the lungs and airways: historical perspective. *J Appl Physiol*. 2006 Aug;101(2):628–34.
- Carr MJ, Udem BJ. Bronchopulmonary afferent nerves. *Respirology*. 2003;8(3):291–301.
- Siniaia MS, Young DL, Poon CS. Habituation and desensitization of the Hering-Breuer reflex in rat. *J Physiol*. 2000;523(2):479–91.
- Mughrabi IT, Hickman J, Jayaprakash N, Thompson D, Ahmed U, Papadoyannis ES, et al. Development and characterization of a chronic implant mouse model for vagus nerve stimulation. *eLife*. 2021 Apr 6;10:e61270.
- Ahmed U, Chang YC, Cracchiolo M, Lopez MF, Tomaiolo JN, Datta-Chaudhuri T, et al. Anodal block permits directional vagus nerve stimulation. *Sci Rep*. 2020 Jun 8;10(1):9221.
- McAllen RM, Shafton AD, Bratton BO, Trevaks D, Furness JB. Calibration of thresholds for functional engagement of vagal a, B and C fiber groups in vivo. *Bioelectron Med*. 2018 Jan 1;1(1):21–7.
- Parker JL, Shariati NH, Karantonis DM. Electrically evoked compound action potential recording in peripheral nerves. *Bioelectron Med*. 2018 Jan 1;1(1):71–83.
- Vuckovic A, Tosato M, Struijk JJ. A comparative study of three techniques for diameter selective fiber activation in the vagal nerve: anodal block, depolarizing prepulses and slowly rising pulses. *J Neural Eng*. 2008 Sep 1;5(3):275–86.
- Grill WM, Mortimer JT. Inversion of the current-distance relationship by transient depolarization. *IEEE Trans Biomed Eng*. 1997 Jan;44(1):1–9.
- Hennings K, Arendt-Nielsen L, Andersen OK. Orderly activation of human motor neurons using electrical ramp prepulses. *Clin Neurophysiol*. 2005 Mar 1;116(3):597–604.
- Hennings K, Arendt-Nielsen L, Christensen SS, Andersen OK. Selective activation of small-diameter motor fibres using exponentially rising waveforms: a theoretical study. *Med Biol Eng Comput*. 2005;43(4):493–500.
- Fang ZP, Mortimer JT. Selective activation of small motor axons by quasitrapezoidal current pulses. *IEEE Trans Biomed Eng*. 1991;38(2):168–74.
- Fang ZP, Mortimer JT. A method to effect physiological recruitment order in electrically activated muscle. *IEEE Trans Biomed Eng*. 1991 Feb;38(2):175–9.
- Muzquiz MI, Mintch L, Horn MR, Alhawwash A, Bashirullah R, Carr M, et al. A reversible low frequency alternating current nerve conduction block applied to mammalian autonomic nerves. *Sensors*. 2021 Jan;21(13):4521.
- Mintch LM, Muzquiz I, Horn MR, Carr M, Schild JH, Yoshida K. Reversible conduction block in peripheral mammalian nerve using low frequency alternating current. In: 2019 9th international IEEE/EMBS conference on neural engineering (NER); 2019. p. 823–4.
- Muzquiz MI. Reversible nerve conduction block using low frequency alternating currents [Internet]. [Thesis]. 2020. Available from: <https://scholarworks.iupui.edu/handle/1805/23576>
- Muzquiz MI, Richardson L, Vetter C, Smolik M, Alhawwash A, Goodwill A, et al. In-vivo application of low frequency alternating currents on porcine cervical vagus nerve evokes reversible nerve conduction block. *Bioelectron Med*. 2021 Dec;7(1):9.
- Pelot NA, Grill WM. In vivo quantification of excitation and kilohertz frequency block of the rat vagus nerve. *J Neural Eng*. 2020 Mar 9;17(2):026005.
- Kilgore KL, Bhadra N. Reversible nerve conduction block using kilohertz frequency alternating current. *Neuromodulation J Int Neuromodulation Soc*. 2014 Apr;17(3):242–55.
- Hopfinger JB, Parsons J, Fröhlich F. Differential effects of 10-Hz and 40-Hz transcranial alternating current stimulation (TACS) on endogenous versus exogenous attention. *Cogn Neurosci*. 2017 Apr 3;8(2):102–11.



30. Rukwied R, Thomas C, Obreja O, Werland F, Kleggetveit IP, Jorum E, et al. Slow depolarizing stimuli differentially activate mechanosensitive and silent C nociceptors in human and pig skin. *PAIN* [Internet]. 2020;161(9):2119–28. Available from: [https://journals.lww.com/pain/Fulltext/2020/09000/Slow\\_depolarizing\\_stimuli\\_differentially\\_activate.18.aspx](https://journals.lww.com/pain/Fulltext/2020/09000/Slow_depolarizing_stimuli_differentially_activate.18.aspx)
31. Ward AR, Shkuratova N. Russian electrical stimulation: the early experiments. *Phys Ther*. 2002 Oct 1;82(10):1019–30.
32. Cogan SF. Neural stimulation and recording electrodes. *Annu Rev Biomed Eng*. 2008 Aug;10(1):275–309.
33. Rattay F. Analysis of models for external stimulation of axons. *IEEE Trans Biomed Eng*. 1986 Oct;BME-33(10):974–7.
34. National Research Council. Guide for the care and use of laboratory animals: eighth edition [Internet]. Washington, DC: The National Academies Press; 2011. 246 p. Available from: <https://www.nap.edu/catalog/12910/guide-for-the-care-and-use-of-laboratory-animals-eighth>
35. Richardson L, Ahmed C, Smolik M, Yoshida K. 3D printed hinged multi-contact cuff electrodes for rapid prototyping and testing. In: 22 Annual Conference of The International Functional Electrical Stimulation Society (IFESS). Nottwil, Switzerland; 2018. p. 123–6.
36. Chang RB, Strohlic DE, Williams EK, Umans BD, Liberles SD. Vagal sensory neuron subtypes that differentially control breathing. *Cell*. 2015 Apr 23;161(3):622–33.
37. Horn MR, Alhawwash A, Yoshida K. In-vivo measurement of the Block Activation Window for sinusoidal Low Frequency Alternating Current (LFAC) stimulation. In: 24th Biennial Congress of the International Society of Electrophysiology and Kinesiology (ISEK). Québec City, PQ, Canada; 2022. p. 144.
38. Lazorchak N, Horn MR, Muzquiz MI, Mintch L. Accurate simulation of cuff electrode stimulation predicting in-vivo strength-duration thresholds. Abstracts from the IFESS 2021 conferences; 2022. p. E33–210.
39. Rattay F. Analysis of models for extracellular fiber stimulation. *IEEE Trans Biomed Eng*. 1989 Jul;36(7):676–82.
40. Horn MR, Ahmed C, Yoshida K. Low frequency alternating current block—a new method to stop or slow conduction of action potentials. In: 2019 9th international IEEE/EMBS conference on neural engineering (NER); 2019. p. 787–90.

**How to cite this article:** Alhawwash A, Muzquiz MI, Richardson L, Vetter C, Smolik M, Goodwill A, et al. In vivo peripheral nerve activation using sinusoidal low-frequency alternating currents. *Artif Organs*. 2022;46:2055–2065. <https://doi.org/10.1111/aor.14347>